Excerpt from the Proceedings of the 2011 COMSOL Conference in Stuttgart

Coupling between mass density and director arrangement in Nematic Liquid Crystals

G. Rosi[1,2], L. Teresi[1,2], F. dell'Isola[2,3], A. DiCarlo[1,2]

[1] LaMS - Modeling & Simulation Lab,
Università Roma Tre, Via Corrado Segre 6, Rome, Italy
[2] Dipartimento di Ingegneria Strutturale e Geotecnica,
Università di Roma La Sapienza, Via Eudossiana 18, 00146 Rome, Italy
[3] International Research Center on Mathematics and Complex Systems,
Università degli Studi dell'Aquila, Palazzo Caetani, 04012, Cisterna di Latina (LT), Italy

Abstract: We present a model which predicts the possibility of inducing pressure waves in Nematic Liquid Crystals (NLCs), enclosed in an electrical wave-guide, by means of a suitable periodic electric potential applied at the electrodes. By proposing a novel interaction term which includes the coupling between mass density, director and gradient of director fields, we predict that a periodic voltage with the appropriate amplitude can lead to the sought-after acoustic resonance in NLCs. Our numerical simulations show that this constitutive assumption leads to results in agreement with previous experimental measures; moreover, our results could serve as a guidance to design further experiments.

1 Introduction

Liquid crystals - as all liquids - are generally modelled as incompressible media. And rightly so, since mass-density changes occurring in these mesophases are minuscule and inconsequential in most regimes of interest. However, liquid crystals exhibit also phenomena such as acousto-optic and acousto-electric interactions that call for a more refined theory. In particular, it has been experimentally established that the Freedericksz transition triggered in a Nematic Liquid-Crystal (NLC) sample by an electrical pulse generates an audible acoustic signal[1]. With the aim of explaining this phenomenon, and the converse effect of perturbing the directors orientation by means of an applied acoustic wave, some attempts are present in the literature, as in Selinger and its co-workers [2, 4, 3, 5], where an interaction energy proportional to the nematic orientation $\mathbf{n} \otimes \mathbf{n}$ and the gradient of the density ρ is proposed; more recently Virga [6, 7], to capture nemato-acoustic phenomena, modelled the NLC as a second gradient fluid. What we are proposing in this work is still the introduction of an interaction energy between the fluid density and the nematic orientation. Our model is based on the assumption that the molecules of the NLCs are mostly packed when the nematic mesogen stay aligned, and that this configuration yields a maximum for the density of the NLCs. Thus, for a given pressure, density varies when neighboring mesogens are oriented along different directions; in particular, an orientation gradient yields "loosely packed" mesogens, and consequently, fluid has a lower density. Few words are needed to present our ansatz: we assume that when the directors of the nematic fluid are all parallel, then the molecules of the fluid are all packed in the most "ordered way". Therefore in this configuration the density of the liquid crystal attains its maximum value. When close material particles of the liquid crystals have directors oriented in different directions, once fixed the liquid pressure, the density varies depending on the assumed directors' configuration. This occurs because the molecules of the fluid crystal, in presence of gradients of orientation, are more "loosely packed" and consequently the density is lower.

2 Theory

Here, we will present an interaction energy based on our assumption, and show through numerical simulations a series of results in agreement with experimental measures, highlighting the possibility of generating pressure waves by means of an applied electric potential. Denoted with $\mathbf{r}$ its position vector, the material particle is in a state characterized by: the nematic director $\mathbf{n}(\mathbf{r})$, the density $\rho(\mathbf{r})$, the electric field $\mathbf{E}(\mathbf{r})$, and the velocity $\mathbf{v}(\mathbf{r})$; the dependence on the position will be omitted unless needed. It is important to remind that for NLCs, the states corresponding to $\mathbf{n}$ and $-\mathbf{n}$ are indistinguishable[10]. We will base our modelling procedure on the introduction of the following specific energy density:

$$e = e_F(\mathbf{n}, \nabla\mathbf{n}) + e_E(\mathbf{E}, \mathbf{n}) + e_A(\rho, \mathbf{v}) + e_I(\rho, \mathbf{n}, \nabla\mathbf{n}) \tag{1}$$

where one can easily identify e_F, e_E, e_A and e_I as the Frank-Oseen, electro-static, acoustic and (newly introduced) interaction specific energy densities, respectively. As extensively described in the literature [10], one can assume:

$$e_F = \frac{1}{2} K \left\|\nabla\mathbf{n}\right\|^2, \qquad e_A = e_C + \frac{1}{2}\mathbf{v}^2, \tag{2a}$$

$$e_E = -\frac{1}{2}\varepsilon_\perp \mathbf{E}\cdot\mathbf{E} - \frac{1}{2}\varepsilon_a \left(\mathbf{E}\cdot\mathbf{n}\right)^2, \tag{2b}$$

where $\varepsilon_\perp$ is the specific transverse dielectric constant, ε_a is the specific dielectric anisotropy, and K is the specific Frank elastic constant in the one constant approximation and e_C the specific elastic energy describing compressibility in a NLC. Also the considered specific interaction energy will need to verify objectivity conditions, exactly as must be required to Frank-Oseen energy. Therefore using the representation theorems presented in [8, 9] we have

$$e_I(\rho, \mathbf{n}, \nabla\mathbf{n}) = e_I(\rho, \nabla\cdot\mathbf{n}, \nabla_\perp\mathbf{n}, \nabla\mathbf{n}\cdot\mathbf{n}), \tag{3}$$

where $\nabla\mathbf{n}_\perp = \nabla\mathbf{n} - \nabla\mathbf{n}\cdot\mathbf{n}\otimes\mathbf{n}$. The importance of the specific interaction energy we have just introduced will be illustrated by considering what appears to be its simplest form

$$\rho\, e_I = s(\mathbf{n}, \nabla\mathbf{n}) \tag{4}$$

$$s(\mathbf{n}, \nabla\mathbf{n}) := \alpha_{\mathbf{1}}\|\nabla\cdot\mathbf{n}\|^{\mathbf{2}} + \alpha_{\mathbf{2}}\|\nabla_\perp\mathbf{n}\|^{\mathbf{2}} + \alpha_{\mathbf{3}}\|\nabla\mathbf{n}\cdot\mathbf{n}\|^{\mathbf{2}} \tag{5}$$

where α_i will be interpreted as dilatation coefficients. Indeed some physical considerations are needed now: the specific interaction energy term is intended to describe volume changes induced, in a nematic fluid, by the spatial gradient of the field $\mathbf{n}$. The main idea which has suggested Eq. (4) is the following: for a fixed specific volume $1/\rho$ and for increasing norms of $\nabla\mathbf{n}$ this energy is expected to increase. As a consequence of Eqs.(2), (4) one gets

$$p = \rho^2 \frac{\partial e}{\partial \rho} = \rho^2 \frac{\partial e_C}{\partial \rho} - s. \tag{6}$$

When it can be linearised in the neighbourhood of the value $\overline{\rho}$, Eq. (6) reads

$$p = \overline{p} + c_o^2(\rho - \overline{\rho}) - s =: \overline{p} + c_o^2(\rho - \rho^*) \tag{7}$$

where c_o is the speed of sound in considered NLC. In order to give a suggestive interpretation of the newly introduced mass density ρ^* we may interpret the coefficients α_i/c_o^2, $i = 1...3$ as the variations of the nematic fluid mass density (which corresponds to the pressure $\overline{p}$) induced by the nematic distortion respectively corresponding to $\|\nabla\cdot\mathbf{n}\|$, $\|\nabla_\perp\mathbf{n}\|$ and $\|\nabla\mathbf{n}\cdot\mathbf{n}\|$. In other words, when the nematic fluid is in the spherical stress state described by the pressure $\overline{p}$, then the relative mass density assumes the value ρ^* (which depends on $\mathbf{n}$ and $\nabla\mathbf{n}$ as specified by Eq. (6)). In the present

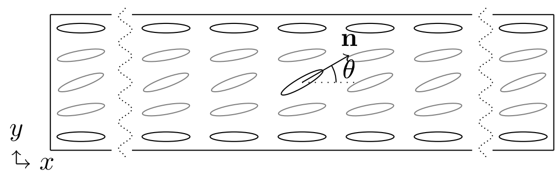

Figure 1: Geometry of the cell.

paper we will limit ourselves to consider dilatation coefficients α_i such that in any considered static and dynamic regimes

$$\sup_{\mathbf{r}\in\mathcal{D}} s \ll c_o^2\,\overline{\rho}. \tag{8}$$

Let $\mathcal{D}$ be a rectangular region of the cartesian plane with sides parallels to the coordinate axes x and y, as in Fig 1. The boundary $\partial\mathcal{D}$ is partitioned in the upper and lower electrodes, $\partial\mathcal{D}^+$ and $\partial\mathcal{D}^-$, respectively, both parallels to x, and the two sides electrodes $\partial\mathcal{D}^\parallel$, parallels to y. In this 2D case, the orientation of nematic director $\mathbf{n}$ may be described by the angle θ it forms with a horizontal direction, thus, $\mathbf{n} = (\cos\theta, \sin\theta)$. In our reduced geometry, taking into account the strong anchoring conditions at the boundaries, Eq.(2) reads as

$$e_F = \frac{1}{2}K\,(\nabla\theta)^2\,, \qquad e_A = e_C + \frac{1}{2}\mathbf{v}^2\,, \tag{9a}$$

$$e_E = -\frac{1}{2}\,\varepsilon_a\,(E_x\cos\theta + E_y\sin\theta)^2\,, \tag{9b}$$

and Eq.(5) reduces to

$$s = \alpha_1\,(\cos\theta\theta_{,y} - \sin\theta\theta_{,x})^2 + \alpha_3\,(\cos\theta\theta_{,x} + \sin\theta\theta_{,y})^2\,.$$

where α_2 plays no role as a consequence of the 2D geometry of the considered case of study. When a voltage $V(t)$ is applied at the top side of a nematic sample, while grounding the opposed side, the so called Freedericksz transition can be triggered[10]. When $|V(t)|$ is below a given threshold, the only solution for nematic orientation is $\theta = 0$; above this threshold, a bifurcation of the type called "pitchfork supercritica" occurs. Indeed, when $|V(t)|$ exceeds the critical value, three configurations are possible: the trivial one is unstable; the other two, symmetric with respect to each other, are both stable.

3 Governing Equations

The non-dimensional equations of motion obtained from Eqs.(9) are:

$$\Delta\theta - \frac{\pi^2}{2}\left[(\tilde{E}_x^2 - \tilde{E}_y^2)\sin 2\theta - \tilde{E}_x\tilde{E}_y\cos 2\theta)\right] = 0\,, \tag{10a}$$

$$\nabla\cdot\left(\varepsilon_\perp\tilde{\mathbf{E}} + \varepsilon_a\left(\tilde{\mathbf{E}}\cdot\mathbf{n}\right)\mathbf{n}\right) = 0\,, \tag{10b}$$

$$\tilde{\mathbf{E}} + \nabla v = 0\,, \tag{10c}$$

$$\Delta\tilde{p} - \tilde{p}_{,tt} = -\gamma\tilde{s}_{,tt}\,, \tag{10d}$$

where the non-dimensional coupling coefficient appearing in Eq.(10d) is given by

$$\gamma = \frac{K}{4\,p_o\,l_o^2}. \tag{11}$$

The other normalized quantities are given by $\tilde{\rho} = \rho/\rho_o$, $\tilde{p} = (p - \overline{p})/p_o$, $\tilde{s} = s\,l_o^2/K$, $\tilde{u} = u\,l_o^2/\alpha_0$, $\tilde{t} = t/t_o$ and $\tilde{\mathbf{e}} = \mathbf{E}/E_o$ where p_o, ρ_o, l_o and E_o are suitable scaling quantities; moreover, $v = V/V_o$ is the non-dimensional voltage, with $V_o = \pi\sqrt{K/\varepsilon_a}$. The characteristic time and electric field are $t_o = l_o/c_o$, and $e_o = /l_o$, with l_o the side length along y. Strong anchoring conditions are imposed at the boundaries $\partial\mathcal{D}^+$ and $\partial\mathcal{D}^-$, while $\partial\theta/\partial x = 0$ is set at $\partial\mathcal{D}^\parallel$. Finally, a hard wall condition for the pressure field is considered on whole $\partial\mathcal{D}$.

4 Numerical Model

Because of the multi-physics nature of the model, three pairwise-coupled physics from three different modules are used:

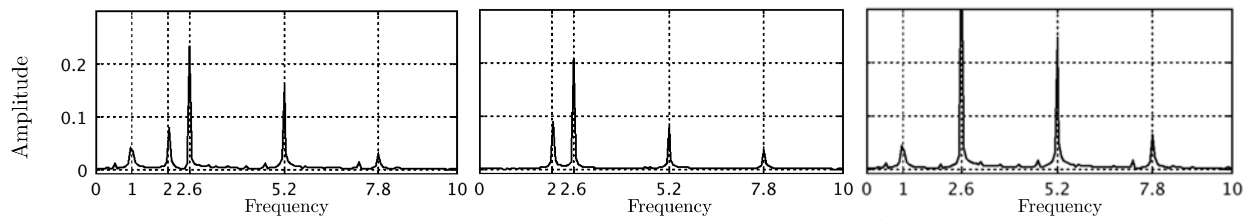

(a) Forced response $\alpha_1 = \alpha_o$, $\alpha_3 = 0$ (b) Forced response $\alpha_1 = 0$, $\alpha_3 = \alpha_o$ (c) Forced response $\alpha_1 = \alpha_o$, $\alpha_3 = \alpha_o$

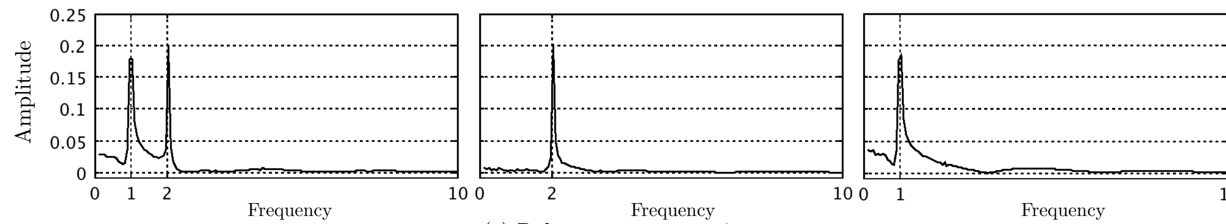

(d) Pulse response $\alpha_1 = \alpha_o$, $\alpha_3 = 0$ (e) Pulse response $\alpha_1 = 0$, $\alpha_3 = \alpha_o$ (f) Pulse response $\alpha_1 = \alpha_o$, $\alpha_3 = \alpha_o$

Figure 2: FFTs of the pressure corresponding to an applied electric signal which crosses the threshold. The other parameters of the simulations are: $v_0 = 1.2$, $\tilde{f}_f = 1.3$, $\alpha_o = 10^{-8}$ J/Pa, $f_o = 1.572$ MHz

(i) Electrostatics from the AC/DC Module - coupled with (iii) - for computing the electric potential

(ii) Transient Pressure Acoustics from the Acoustic Module - coupled with (iii) - for computing the pressure;

(iii) Weak-form PDE from the Mathematics Module -coupled with (i) -for computing the nematic director field

The pressure response of the nematic liquid-crystal cell to a voltage input is then computed by performing a time-dependent analysis with a BDF solver, taking care of satisfying by the Courant-Friedrichs-Lewy condition. The evolutive solver is initialized with the fields obtained from the stationary solution under a given voltage. This allows the solver to overcome the difficulties due to the violent nonlinearities triggered by the crossing of the Freedericksz threshold. The fast Fourier transform of the output signal is finally computed for a number of input signals and for different values of the coupling parameters.

5 Experimental results

In our numerical simulations we consider as reference configuration for the NLC an electrically unperturbed specimen with spatially constant pressure field; the non-dimensional Freedericksz threshold is $v_F = 1$. We then apply on the upper side $\partial\mathcal{D}^+$ two kinds of time variable electric potential:

(a) a harmonic signal $V(t) = v_0 \sin(2\pi \tilde{f}_f \tilde{t})$

(b) a rectangular pulse of amplitude V_0 and length $\tilde{t}_f$;

We assume $v_0 > v_F = 1$, thus large enough to realize a Freedericksz transition. The Fast Fourier Transforms (FFTs) of the pressure signal are plotted in Fig.2. The FFTs of the forced response, Figures 2a, 2b, and 2c, exhibit strong components at $2\tilde{f}_f$, $4\tilde{f}_f$ and $6\tilde{f}_f$, together with the cavity modes at $\tilde{f} = 1, 2$, while no signal is detected at f_f. These high order harmonics of the forcing signal are due to the non linearity of the system, and in particular to the crossing of the threshold, and

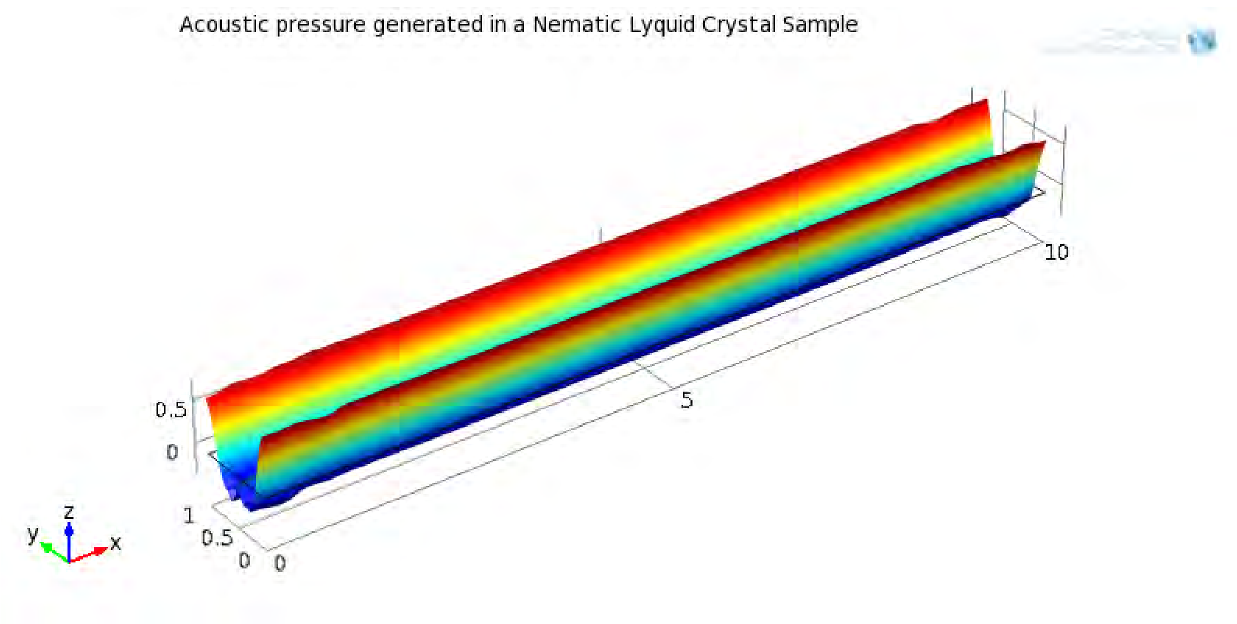

Figure 3: Pressure field generated in a NLC

are in agreement with the experiments[1]. The FFTs of the pulse response, Figures 2d, 2e and 2f, show the presence of the cavity modes at $\tilde{f} = 1$, $\tilde{f} = 2$, and highlight the fact that their excitation depends on the values of α_1 and α_3. In Figure 3 the pressure field generated in the NLC is shown. The reference configurations we used in the numerical simulations all have vanishing velocity fields: future investigations should involve the study of the effects on wave propagation induced by stationary, non vanishing velocity fields in the reference configurations.

6 Conclusions

As shown, the mechanical balance equations show some interesting features, in particular the switch induced by the Freedericksz transition may change in a relevant way the overall behaviour of the induced waves. Future investigations on this phenomenon can lead to the establishment of an experimental procedure for measuring these coefficients or for controlling the actual response of NLCs to a pulse excitation.

References

[1] YJ K and JS Patel. *Applied Physics Letters*, **75**(13) 1985-1987 (1999).

[2] VA Greanya, AP Malanoski, BT Weslowski, MS Spector, and JV Selinger. *Liquid Crystals*, **32**(7) 933941 (2005).

[3] VA Greanya, MS Spector, JV Selinger, BT Weslowski, and R Shashidhar. *Journal of Applied Physics*, **94**(12) 75717575 (2003).

[4] A Malanoski, VA Greanya, B Weslowski, MS Spector, JV Selinger, and R Shashidhar. *Physical Review E*, **69** 021705 (2004).

[5] JV Selinger, MS Spector, VA Greanya, B Weslowski, D Shenoy, and R Shashidhar. *Physical Review E*, **66**(5) 051708 (2002).

[6] EG Virga. *Physical Review E*, **80** 031705 (2009).

[7] G de Matteis and Epifanio G. Virga. *Physical Review E*, **83**(1) 011703 (2011).

[8] CC Wang. *Archive for Rational Mechanics and Analysis*, **36**(3) 166-197 (1970).

[9] I W Stewart. *The Static and Dynamic Continuum Theory of Liquid Crystals* (2004).

[10] Iam-Choon Khoo. *Liquid crystals.* Wiley-Blackwell (2007).